Coarsening of Reverse Tilt Domains in Liquid-Crystal Cells with Heterogeneous Alignment Layers

D. K. Shenoy, J. V. Selinger, K. A. Grüneberg, J. Naciri, and R. Shashidhar

Center for Bio/Molecular Science and Engineering, Naval Research Laboratory,
Code 6900, 4555 Overlook Avenue, SW, Washington, DC 20375
(Received 15 October 1998)

When an electric field above the Fréedericksz threshold is applied to a nematic liquid crystal in a cell with heterogeneous alignment layers, the system exhibits reverse tilt domains. Over a time scale of seconds to minutes, the disordered domain pattern coarsens into a uniform texture. Analysis of the coarsening dynamics shows that the characteristic length scale L grows with time t as $L \sim (\log t)^4$. This scaling is consistent with predictions of the random-bond Ising model, in which randomness in the Ising bond strength represents heterogeneity in the alignment layers. [S0031-9007(99)08519-1]

One of the main concerns of nonequilibrium statistical mechanics is coarsening, the dynamic growth of domains after a system is quenched into an ordered phase. Experimentally, coarsening has often been studied in liquid-crystal systems [1–7]. Liquid crystals are particularly well suited to these studies because the length and time scales of domain growth are accessible to experiments and because the growth of domains can easily be monitored in microscope images. However, one limitation of experimental studies of coarsening in liquid crystals has been that they have only investigated coarsening in uniform systems; they have not investigated the effects of quenched disorder. This is a significant limitation, because quenched disorder is predicted to have major effects on coarsening dynamics [8].

In this paper, we present a study of coarsening of reverse tilt domains in a nematic liquid crystal in a narrow cell [9], with alignment layers prepared through a new process of chemisorption and photoinduced dimerization [10]. Depending on the preparation conditions, the alignment layers can be either homogeneous or heterogeneous. Hence, this system allows us to investigate the effects of quenched disorder in the alignment layers on the coarsening of reverse tilt domains. Theoretically, the system of reverse tilt domains maps onto the Ising model, and heterogeneity in the alignment layers might correspond to either random-field or random-bond disorder in the Ising model. Experimentally, the coarsening data generally give a good fit to the predictions of the random-bond Ising model—a better fit than to the predictions of either the random-field or the uniform Ising model. Thus, these results provide experimental confirmation of theoretical predictions for domain growth under conditions of quenched random-bond disorder.

Our experimental geometry is shown in Fig. 1. The nematic liquid crystal mixture ZLI 4792 (Merck) is confined at room temperature in a 20-μm-thick planar cell with aligning surfaces that anchor the molecular director in the surface plane in the $\pm x$ direction. When an electric field above the Fréedericksz threshold is applied perpendicular to the surfaces, the director tilts out of the surface plane. As shown in Fig. 1(a), the director can tilt in two possible orientations, which are approximately degenerate in energy. These two orientations will be called the $(+)$ and $(-)$ states of the system. Hence, the system can break into $(+)$ and $(-)$ domains, called reverse tilt domains, as shown in the top view of Fig. 1(b). Because of the difference in the Frank elastic constants for bend and twist distortions of the director, the domain-wall line tension is anisotropic, and hence the domains are elongated.

We prepare the surfaces with a new nonrubbing technique [10], which can produce alignment layers with different levels of heterogeneity. In this technique, a monolayer is chemisorbed onto the surface and then exposed to linearly polarized ultraviolet light. The polarization of the light selects a favored axis of dimerization within the monolayer, and the nematic director is anchored perpendicular to this favored axis. In a first group of alignment layers, prepared without special efforts to obtain uniform surfaces, there are several types of surface heterogeneity, including dust particles, substrate roughness, and nonuniform surface coverage. In a later group of alignment layers, all of these types of surface heterogeneity are controlled through careful preparation in the clean room.

The preparation conditions of the alignment layers determine whether the cell forms reverse tilt domains.
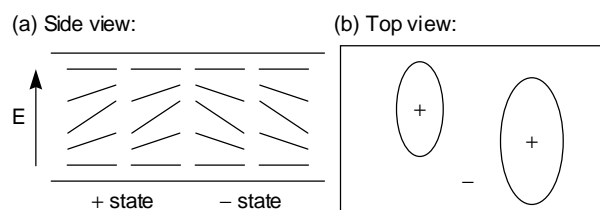
FIG. 1. Geometry of reverse tilt domains in a narrow cell of nematic liquid crystal. (a) Side view. (b) Top view.

When heterogeneous alignment layers are used, the cell forms a disordered pattern of reverse tilt domains, as shown in Figs. 2 and 3. This pattern coarsens into a uniform director field over a time scale of seconds to minutes. When the field is removed and then applied again, the cell forms approximately the same pattern of domains in approximately the same locations. This reproducibility shows that certain sites on the heterogeneous surface favor the nucleation of reverse tilt domains. By contrast, when homogeneous alignment layers prepared in the clean room are used, the cell does not form reverse tilt domains. This result is further evidence that surface heterogeneity is important for reverse tilt domains. As an additional test, the homogeneous alignment layers prepared in the clean room were placed into cells with brittle glass spacers that fractured under compression, creating a different type of heterogeneity. Those cells formed reverse tilt domains,

confirming that the nucleation of this domain structure depends on surface heterogeneity.

Because surface heterogeneity is important for reverse tilt domains in these cells, this system provides us with an opportunity to examine the dynamics of coarsening in the presence of heterogeneity. In particular, it allows us to test theoretical predictions for coarsening in heterogeneous systems. The predictions are based on a mapping of the system onto the two-dimensional Ising model. In this mapping, the $(+)$ and $(-)$ states of the liquid crystal correspond to the Ising spin states $\sigma_i = \pm 1$. The elastic constants of the liquid crystal give the energy cost for domain walls, which corresponds to the Ising exchange constant J. As an approximation, we neglect the anisotropy in J. A cell with homogeneous surfaces then maps onto

FIG. 2. Top: contraction of a single reverse tilt domain. The domain structure is shown in images taken every 35 sec. Bottom: data for the domain-wall perimeter, determined by the number of black pixels in excess of the background level. The data are fit to the prediction of Eq. (4).
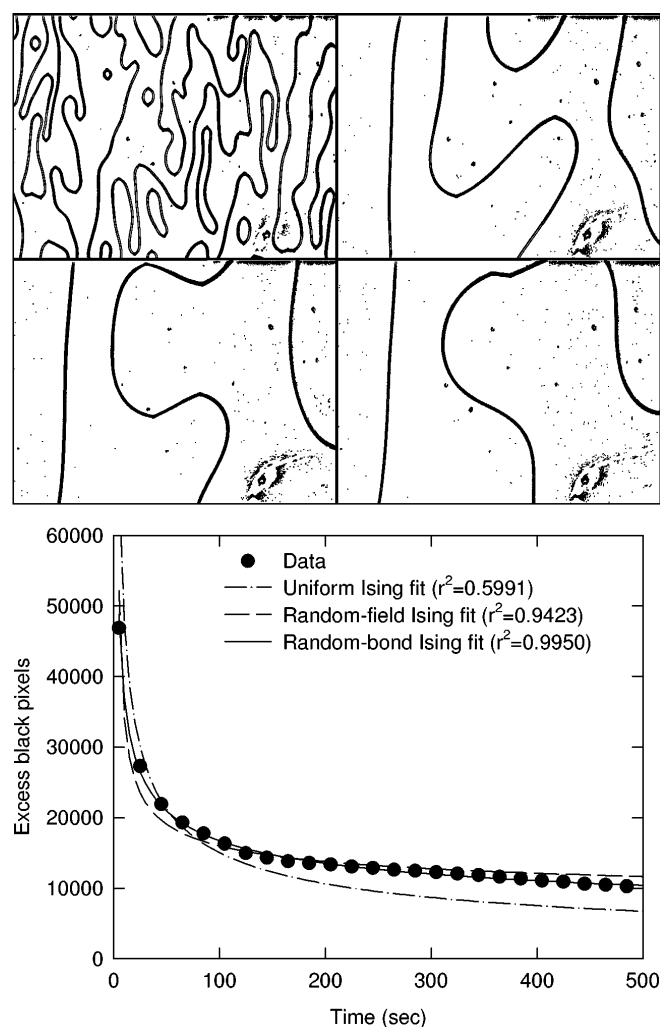
FIG. 3. Top: coarsening of a disordered pattern of many reverse tilt domains, shown at 2, 18, 34, and 50 sec after the electric field is applied. Bottom: data for the total domain-wall perimeter in the field of view, determined by the number of black pixels in excess of the background level. The data are fit to the predictions of the uniform Ising model, the random-field Ising model, and the random-bond Ising model. (For clarity, only every fourth data point is shown.)

the uniform Ising model, with the Hamiltonian

$$H = -J \sum_{\langle i,j \rangle} \sigma_i \sigma_j. \qquad (1)$$

In a cell with heterogeneous surfaces, the disorder might enter the Hamiltonian in two different ways. If the disorder favors the $(+)$ state in certain locations and the $(-)$ state in other locations, then the cell maps onto the *random-field* Ising model. Its Hamiltonian is

$$H = -J \sum_{\langle i,j \rangle} \sigma_i \sigma_j - \sum_i h_i \sigma_i, \qquad (2)$$

where the random field h_i represents the local preference of the surface for the $(+)$ or $(-)$ state. By contrast, if the disorder gives different energy costs for domain walls at different locations (for example, if domain walls are pinned by grains of dust), then the cell maps onto the *random-bond* Ising model. Its Hamiltonian is

$$H = -\sum_{\langle i,j \rangle} J_{ij} \sigma_i \sigma_j, \qquad (3)$$

where $J_{ij} > 0$ represents the local energy cost for domain walls.

There are distinct predictions for coarsening in each of these three models. In the uniform Ising model, coarsening is controlled by the competition between the curvature-induced force, which favors domain-wall motion, and the domain-wall viscosity, which resists this motion. As a result, a single circular domain of radius $R(t)$ contracts following the differential equation $dR/dt = -\Gamma J/R$, where Γ is an inverse viscosity [11]. The solution of this equation gives the prediction

$$R(t) = [R(0)^2 - \Gamma Jt]^{1/2}. \qquad (4)$$

By the same argument, a disordered pattern of domains with the characteristic length scale $L(t)$ coarsens as $L(t) \propto t^{1/2}$. By comparison, in the random-field Ising model, the rate of coarsening is limited by the pinning forces associated with heterogeneity in the random field. As a result, a disordered pattern of domains is predicted to coarsen as $L(t) \propto \log(t/\tau)$, where τ is a characteristic time scale [12]. Finally, in the random-bond Ising model, the rate of coarsening is limited by pinning forces associated with heterogeneity in the random bonds, which are less effective than random-field pinning forces. Hence, the prediction for coarsening in the random-bond Ising model is $L(t) \propto [\log(t/\tau)]^{(2-\zeta)/(d-3+2\zeta)}$, where d is the spatial dimension and ζ is the wall roughness exponent [8]. In $d = 2$, appropriate to our experiment, the value $\zeta = \frac{2}{3}$ is known [8], and hence the prediction for coarsening becomes $L(t) \propto [\log(t/\tau)]^4$.

For a preliminary comparison of the predictions with our experiments, we examined the contraction of a single reverse tilt domain in a region of roughly 1.3 mm across, using a $5\times$ objective on an Olympus BX50WI microscope. Images of 640×484 pixels were acquired

every 5 sec using a Sony CCD camera and digitized using an Oculus TCX/MX frame grabber board (Coreco). The images were processed in Adobe Photoshop 4.0, first using a high-pass filter (radius 10 pixels) to remove nonuniformities in the overall brightness, then using a threshold filter to enhance the domain-wall contrast. Some of the resulting images are shown in Fig. 2. In these images, the domain walls are black and the interiors of both $(+)$ and $(-)$ domains are white, with some extraneous black pixels associated with dirt and other artifacts in the optics. We counted the number of black pixels in each image, then subtracted the background level of black pixels remaining in the final image, after the domain disappeared. This procedure gave the number of excess black pixels, which is proportional to the domain perimeter. This perimeter should scale as the radius predicted by Eq. (4). The data are shown in Fig. 2, along with a fit to the prediction. This fit shows that the Ising model gives a good description of the late stages of domain contraction. The fit does not, however, show whether the uniform, random-field, or random-bond Ising model is the most appropriate for this system, because the late stages of contraction are dominated by a large curvature force (scaling as R^{-1}), which exceeds any random-field or random-bond pinning force.

To determine which version of the Ising model is the most appropriate for this experimental system, one must examine the coarsening of a disordered pattern of many domains. We took several sequences of images of the coarsening of multidomain patterns, and processed each sequence using the procedure outlined above. Because the domain walls generally did not go away by the final image in the sequence, we determined the background level of black pixels by manually erasing the domain walls from the final image in each sequence using Photoshop. We then subtracted the background level from the number of black pixels in each image to obtain the number of excess black pixels, which is proportional to the total domain perimeter within the field of view. This total domain perimeter can be related to the coarsening length scale $L(t)$: Because the number of domains in the field of view scales as L^{-2}, and the perimeter of each domain scales as L, the total domain perimeter must scale as L^{-1} [13]. Hence, the data can be compared with the predictions for L^{-1} from each version of the Ising model. Specifically, we fit the number of excess black pixels $P(t)$ to the following functions: for the uniform Ising model

$$P(t) = c(t - \tau)^{-1/2}, \qquad (5)$$

for the random-field Ising model

$$P(t) = c[\log(t/\tau)]^{-1}, \qquad (6)$$

and for the random-bond Ising model

$$P(t) = c[\log(t/\tau)]^{-4}. \qquad (7)$$

Each of these fits has two parameters, the overall coefficient c and the characteristic time scale τ.

One example of the coarsening data is shown in Fig. 3. In this example, a square wave from a Wavetek Model 395 waveform generator with an amplitude of 6 V (3.2 times the Fréedericksz threshold) and a frequency of 30 Hz was applied to the cell. At early times, the system has a disordered pattern of many reverse tilt domains. After a few seconds, most of the small domains in the field of view contract away, and the system is left with a few large domains, which continue to coarsen by reducing the domain-wall curvature. The plot of the number of excess black pixels as a function of time shows that the total domain perimeter decreases rapidly in the initial stage of coarsening, then more slowly in the later stage. The data are fit to the predictions for the uniform Ising model, the random-field Ising model, and the random-bond Ising model. The random-bond Ising model gives the best fit over the full range of time studied.

We analyzed six data sets analogous to Fig. 3. In four of the six, the random-bond Ising model gave a better fit than either of the other models considered; in the other two data sets, the random-field Ising model gave the best fit. Those two anomalous data sets were the earliest and among the smallest data sets collected, so it is reasonable to put less weight on them. Hence, the ensemble of data shows that the random-bond Ising model gives the best fit to the coarsening dynamics. This best fit is independent of the applied electric field, although the overall coarsening rate is faster at higher fields. (This trend can be understood because a higher field gives a greater difference in molecular orientation between the $(+)$ and $(-)$ states, and hence a greater domain-wall energy and a greater driving force for coarsening.)

We attempted to further differentiate among the models by going to longer time scales, until no more domains are visible in the field of view. However, all of the models break down once $L(t)$ grows comparable to the field of view. The dynamics at those long time scales is dominated by a few square-root cusps analogous to Fig. 2, associated with the disappearance of each of the last remaining domains. This finite-size effect is not described by any of the models. In principle, one might further differentiate among the models by going to a larger spatial scale that would encompass more domains. However, it was not feasible to reduce the magnification and expand the field of view within our experimental optics.

From these results, we can draw two conclusions. First, the coarsening of reverse tilt domains in these liquid-crystal cells is controlled by heterogeneity in the alignment layer, which changes the dynamic scaling of $L(t)$. This result is physically reasonable, because we have already established that the nucleation of reverse tilt domains in these cells is also controlled by surface heterogeneity. Second, the heterogeneity takes the form of random-bond rather than random-field disorder; i.e., it gives randomness in the local energy cost for domain walls rather than randomness in the local energetic

preference for $(+)$ or $(-)$ domains. This result is also reasonable, because dust particles or other defects on the surface can easily give locations with a reduced energy cost for domain walls compared with the clean surface. By comparison, it is difficult to see what physical mechanism would give random-field disorder, with a random local preference for the $(+)$ or $(-)$ state.

In summary, this study shows that surface heterogeneity leads to the formation of reverse tilt domains in liquid-crystal cells with photodimerized alignment layers. The ensemble of data for the coarsening dynamics agrees with the predictions of the random-bond Ising model. These results imply that the cells have a disordered surface that favors the presence of domain walls in preferred locations.

[1] R. Pindak *et al.,* Phys. Rev. Lett. **45**, 1193 (1980).
[2] H. Orihara and Y. Ishibashi, J. Phys. Soc. Jpn. **55**, 2151 (1986); T. Nagaya, H. Orihara, and Y. Ishibashi, J. Phys. Soc. Jpn. **56**, 1898 (1987); **56**, 3086 (1987); **59**, 377 (1990); T. Nagaya *et al.,* J. Phys. Soc. Jpn. **60**, 1572 (1991); **61**, 3511 (1992); T. Nagaya, H. Orihara, and Y. Ishibashi, J. Phys. Soc. Jpn. **64**, 78 (1995).
[3] I. Chuang *et al.,* Science **251**, 1336 (1991); I. Chuang, N. Turok, and B. Yurke, Phys. Rev. Lett. **66**, 2472 (1991); R. Snyder *et al.,* Phys. Rev. A **45**, R2169 (1992); B. Yurke *et al.,* Physica (Amsterdam) **178B**, 56 (1992); A. P. Y. Wong, P. Wiltzius, and B. Yurke, Phys. Rev. Lett. **68**, 3583 (1992); A. N. Pargellis *et al.,* Phys. Rev. A **46**, 7765 (1992); A. N. Pargellis, S. Green, and B. Yurke, Phys. Rev. E **49**, 4250 (1994); B. Yurke *et al.,* Phys. Rev. E **56**, R40 (1997).
[4] B. Kim, S. J. Lee, and J.-R. Lee, Phys. Rev. E **53**, 6061 (1996).
[5] C. Liu and M. Muthukumar, J. Chem. Phys. **106**, 7822 (1997).
[6] H. M. Shehadeh and J. P. McClymer, Phys. Rev. Lett. **79**, 4206 (1997).
[7] W. Wang, T. Shiwaku, and T. Hashimoto, J. Chem. Phys. **108**, 1618 (1998).
[8] T. Nattermann and J. Villain, Phase Transit. **11**, 5 (1988); T. Nattermann and P. Rujan, Int. J. Mod. Phys. B **3**, 1597 (1989).
[9] F. Brochard, J. Phys. (Paris) **33**, 607 (1972); L. Léger, Mol. Cryst. Liq. Cryst. **24**, 33 (1973).
[10] R. Shashidhar *et al.,* US Patent No. 5 578 351 (1996); *Digest of the Society for Information Display, Boston, 1997* (Society for Information Display, Santa Ana, 1997) p. 315.
[11] S. M. Allen and J. W. Cahn, Acta Metall. **27**, 1085 (1979).
[12] J. Villain, Phys. Rev. Lett. **52**, 1543 (1984).
[13] In this sense, the total domain perimeter in our system is analogous to the net domain-wall magnetization of a diluted Ising antiferromagnet, which also scales as the inverse of the coarsening domain size. See M. Lederman *et al.,* Phys. Rev. B **48**, 3810 (1993).